

Figure 1. CT of the brain (A), with a bone window, showing an expansile lesion occupying ethmoid cells and containing calcifications, with bone destruction. MRI demonstrated that the lesion was extra-axial, with lobulated contours, located in the upper portion of the nasal cavity, and extended to the anterior cranial fossa, facial sinuses, and orbits. A coronal T2-weighted sequence (B) shows that the expansile lesion presented an isointense signal, although a hyperintense signal (edema) can be seen in the brain parenchyma in the frontal lobe, mainly on the left. An axial diffusion-weighted imaging sequence (C) shows a hyperintense signal (restricted diffusion). A contrast-enhanced coronal T1-weighted sequence (D) shows intense enhancement.

A indicates that the tumor is limited to the nasal cavity; stage B indicates that it involves only the nasal cavity and paranasal sinuses; and stage C indicates that it extends beyond the stage B limits. The staging system proposed by Dulguerov employs the tumor-node-metastasis classification^(3,4).

Bone destruction and calcification within the lesion can be characterized by CT⁽⁵⁾. An MRI scan provides more accurate information on the extent of the tumor, especially in terms of intracranial and orbital involvement. On MRI, the majority of olfactory neuroblastomas present a signal that is (in relation to that of muscle tissue) hypointense in T1-weighted sequences

and hyperintense in T2-weighted sequences, as well as showing intense enhancement in contrast-enhanced sequences^(6,7). MRI is also superior to CT in the evaluation of recurrence after craniofacial resection, because of its greater ability to differentiate fibrous scar tissue from residual or recurring neoplasia⁽⁶⁾. Cysts in the intracranial margin of the tumor have been reported in cases of olfactory neuroblastoma. Another relevant aspect is a dumbbell-like morphology, the tumor mass being divided between the anterior cranial fossa and the nasal cavity, the cribriform plate forming the “waist”⁽⁵⁾.

The main differential diagnoses of olfactory neuroblastoma include: squamous cell carcinoma, typically in the maxillary antrum, with bone erosion; sinonasal adenocarcinoma, with heterogeneous enhancement, which has been associated with occupational exposure to wood dust; undifferentiated sinonasal carcinoma, which affects older patients; and dural-based invasive meningioma, with poorly defined borders and areas of necrosis⁽⁸⁾.

REFERENCES

1. Ferreira MCF, Tonoli C, Varoni ACC, et al. Estesioneuroblastoma. *Rev Ciênc Méd.* 2007;16:193–8.
2. Howell MC, Branstetter BF 4th, Snyderman CH. Patterns of regional spread for esthesioneuroblastoma. *AJNR Am J Neuroradiol.* 2011;32:929–33.
3. Van Gompel JJ, Giannini C, Olsen KD, et al. Long-term outcome of esthesioneuroblastoma: Hyams grade predicts patient survival. *J Neuro Surg B Skull Base.* 2012;73:331–6.
4. Tajudeen BA, Arshi A, Suh JD, et al. Importance of tumor grade in esthesioneuroblastoma survival: a population-based analysis. *JAMA Otolaryngol Head Neck Surg.* 2014;140:1124–9.
5. Mendonça VF, Carvalho ACP, Freitas E, et al. Tumores malignos da cavidade nasal: avaliação por tomografia computadorizada. *Radiol Bras.* 2005;38:175–80.
6. Li C, Yousem DM, Hayden RE, et al. Olfactory neuroblastoma: MR evaluation. *AJNR Am J Neuroradiol.* 1993;14:1167–71.
7. Schuster JJ, Phillips CD, Levine PA. MR of esthesioneuroblastoma (olfactory neuroblastoma) and appearance after craniofacial resection. *AJNR Am J Neuroradiol.* 1994;15:1169–77.
8. Baptista AC, Marchiori E, Boasquevisque E, et al. Comprometimento órbito-craniano por tumores malignos sinonasais: estudo por tomografia computadorizada. *Radiol Bras.* 2002;35:277–85.

Aline de Araújo Naves¹, Luiz Gonzaga da Silveira Filho¹, Renata Etchebehere¹, Hélio Antônio Ribeiro Júnior², Francisco Valtener A. Lima Junior²

1. Universidade Federal do Triângulo Mineiro (UFTM), Uberaba, MG, Brazil.
2. Hospital das Clínicas da Faculdade de Medicina de Ribeirão Preto da Universidade de São Paulo (HCFMRP-USP), Ribeirão Preto, SP, Brazil. Mailing address: Dra. Aline de Araújo Naves. Universidade Federal do Triângulo Mineiro. Avenida Getúlio Guaritá, 130, Nossa Senhora da Abadia. Uberaba, MG, Brazil, 38025-440. E-mail: rdi.alinenaves@gmail.com.

<http://dx.doi.org/10.1590/0100-3984.2015.0206>

Giant ovarian teratoma: an important differential diagnosis of pelvic masses in children

Dear Editor,

An 8-year-old female patient presented with diffuse abdominal pain accompanied by progressive distension. Physical examination revealed a large abdominal mass, predominantly in the mesogastrium, that was depressible and painless on palpation. Ultrasound showed a solid-cystic formation extending from the epigastrium to the hypogastrium, with a calcium component and an air-fluid level (Figure 1). Computed tomography (CT) showed a massive solid-cystic formation, with a fat component and soft tissue, as well as calcifications, measuring 12.6 × 19.2

× 20.8 cm, exerting a significant mass effect, displacing the small intestine, aorta, and inferior vena cava, as well as causing slight compression of the pancreas, kidneys, and ureters, with no apparent signs of infiltration (Figure 2). Intraoperatively, the mass was seen to be adhered to the left fallopian tube and to the greater omentum (Figure 1). The tumor was excised without complications, and the patient was discharged five days later. A follow-up abdominal ultrasound revealed no changes.

The occurrence of an abdominal mass in a child should always be evaluated by a pediatrician. The main differential diagnoses are organomegaly and fecal impaction. When abdominal palpation produces nonspecific findings, further investigation, employing imaging methods, is required⁽¹⁾.

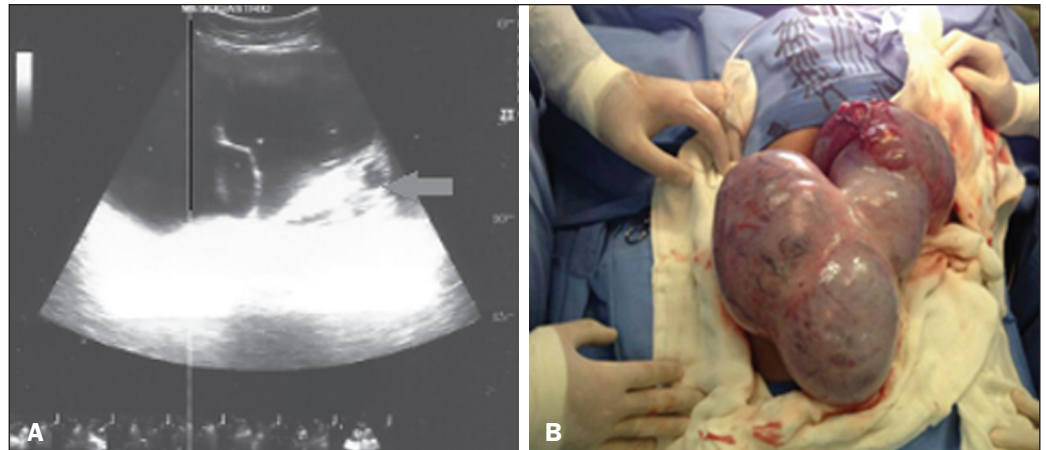


Figure 1. A: Ultrasound of the abdomen, showing a massive solid-cystic formation with a pronounced solid component (arrow). **B:** Intraoperative photograph showing the large volume of the lesion and its encapsulated appearance.

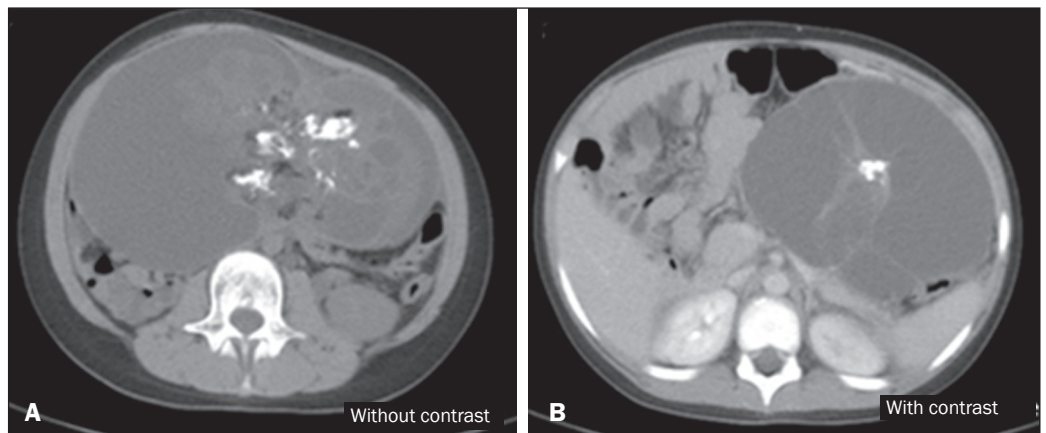


Figure 2. A: Non-contrast-enhanced axial CT scan showing an extensive solid-cystic formation, with a fatty component, a liquid component, and calcifications. **B:** Intravenous contrast-enhanced axial CT scan showing a compressive effect on and displacement of the structures adjacent to the lesion—the pancreas, abdominal aorta, inferior vena cava, small intestine, and left kidney.

Ovarian teratoma is the most prevalent germ cell neoplasm, accounting for approximately 32% of all ovarian neoplasms, and can be divided into mature or immature teratoma depending on its cellular differentiation⁽¹⁾. The cellular components of this lesion are pronounced and varied, potentially encompassing respiratory epithelium, skin, cartilage, mucosa, and neural epithelium^(2–5). It is a benign neoplasm, presenting on physical examination as a palpable pelvic mass, typically 5–10 cm in diameter, and occurs bilaterally in 10–15% of cases⁽¹⁾. In 10% of cases, it is considered an emergency, presenting the typical profile of acute abdomen, due to torsion of the vascular pedicle that occurs secondary to its growth⁽⁶⁾. The clinical diagnoses of abdominal masses are diverse and imprecise, requiring complementary diagnostic imaging⁽⁷⁾.

Abdominal X-ray is nonspecific for ovarian teratoma and can occasionally show calcifications in the area surrounding the lesion. Ultrasound and CT are the main imaging methods for the detection of this disease, the rapid detection of which demands recognition of the typical imaging patterns, particularly in cases of emergency (acute onset). Although CT also has high specificity and sensitivity, particularly for the detection of cystic teratoma, it is not routinely employed, because it involves the use of ionizing radiation. The combination of various imaging methods is an essential part of the surgical planning⁽⁸⁾. The histological study is also of importance, determining the macroscopic and microscopic aspect of the lesion, as well as the prognosis. Surgical treatment—excision of the lesion—is the gold standard⁽⁸⁾.

REFERENCES

1. Wu RT, Torng PL, Chang DY, et al. Mature cystic teratoma of the ovary: a clinicopathologic study of 283 cases. *Zhonghua Yi Xue Za Zhi (Taipei)*. 1996;58:269–74.
2. Akbulut M, Zekioglu O, Terek MC, et al. Florid vascular proliferation in mature cystic teratoma of the ovary: case report and review of the literature. *Tumori*. 2009;95:104–7.
3. Baker PM, Rosai J, Young RH. Ovarian teratomas with florid benign vascular proliferation: a distinctive finding associated with the neural component of teratomas that may be confused with a vascular neoplasm. *Int J Gynecol Pathol*. 2002;21:16–21.
4. Nogales FF, Aguilar D. Florid vascular proliferation in grade 0 glial implants from ovarian immature teratoma. *Int J Gynecol Pathol*. 2002;21:305–7.
5. Fellegara G, Young RH, Kuhn E, et al. Ovarian mature cystic teratoma with florid vascular proliferation and Wagner-Meissner-like corpuscles. *Int J Surg Pathol*. 2008;16:320–3.
6. Stuart GC, Smith JP. Ruptured benign cystic teratomas mimicking gynecologic malignancy. *Gynecol Oncol*. 1983;16:139–43.
7. Mahaffey SM, Ryckman FC, Martin LW. Clinical aspects of abdominal masses in children. *Semin Roentgenol*. 1988;23:161–74.
8. Buy JN, Ghossain MA, Moss AA, et al. Cystic teratoma of the ovary: CT detection. *Radiology*. 1989;171:697–701.

Felipe Nunes Figueiras¹, Márcio Luís Duarte², Élcio Roberto Duarte¹, Daniela Brasil Solorzano¹, Jael Brasil de Alcântara Ferreira¹

1. Santa Casa de Santos – Radiologia, Santos, SP, Brazil. 2. Hospital São Camilo, São Paulo, SP, Brazil. Mailing address: Dr. Felipe Nunes Figueiras. Santa Casa de Santos – Radiologia. Avenida Doutor Cláudio Luís da Costa, 50, Jabaquara. Santos, SP, Brazil, 11075-900. E-mail: bilita88@gmail.com.

<http://dx.doi.org/10.1590/0100-3984.2016.0026>